ELSEVIER

Chemical Engineering Journal 141 (2008) 119–129

Chemical Engineering Journal

www.elsevier.com/locate/cej

Determination of the apparent ozonation rate constants of 1:2 metal complex dyestuffs and modeling with a neural network

Ensar Oguz [a,*], Bülent Keskinler [b], Ahmet Tortum [c]

[a] *Atatürk University, Environmental Engineering Department, 25240 Erzurum, Turkiye*

[b] *Gebze Institute of Technology, Environmental Engineering Department, 41400 Çayırova, Kocaeli, Turkiye*

[c] *Atatürk University, Civil Engineering Department, 25240 Erzurum, Turkiye*

Received 21 March 2007; received in revised form 1 November 2007; accepted 2 November 2007

Abstract

In this study, the apparent ozonation rate constants of 1:2 metal complex dyestuffs under different empirical conditions such as dye concentrations (400–1000 ppm), ozone–air flow rates (5–15 l min^{-1}), the percentages of O_3 in the ozone–air flow rate (0.7–1.4), pH (3–12), temperatures (18–70 °C), powder activated carbon (PAC) (0.5–1.5 g in solution of 250 ml), HCO_3^- (0–26 mM) and H_2O_2 concentrations (0–21 mM) were determined. The ozonation of 1:2 metal complex dyestuffs was found to be fit pseudo-first-order reaction, and the apparent rate constants did not change with the increase of dyestuffs concentrations. For 1:2 metal complex dyestuffs, the apparent rate constants of dyestuffs degradation by ozonation increased with the augmentation of initial pH, H_2O_2, the percentage of O_3 in the ozone–air flow rate and PAC dosage in the solution, but decreased with the increase of HCO_3^- concentration and temperature of the solution. The apparent rate constant of dyestuffs degradation by ozonation increased with the augmentation of ozone–air flow rate from 5 to 10 l min^{-1}, but it did not change in the range of 10–15 l min^{-1}. At a high pH, the ozonation of 1:2 metal complex dyestuffs contributed to the increase the apparent rate constant due to the occurrence of hydroxyl free radicals. Using Arrhenius equation, the activation energy (E_a) of the reaction was found as 3 kJ mol^{-1}. The reaction of the ozonation of the dyestuffs under the different temperatures (291, 313 and 343 K) was defined as diffusion controlled according to E_a. The model based on artificial neural network (ANN) could predict the concentrations of the dyestuffs removal from the aqueous solution during ozonation under the different conditions. A relationship between the predicted results of the designed ANN model and the experimental data was also conducted. The ANN model yielded a determination coefficient of $R^2 = 0.978$, a standard deviation ratio of 0.146, a mean absolute error of 19.503 and a root mean square error of 56.600.

Keywords: Ozonation; Apparent rate constant; Neural network; Dyestuffs

1. Introduction

Ozone can oxidize organics and inorganics to their highest oxidation states, depending on the molecular selectivity and decay rates [1]. The disintegration rate of ozone is affected by temperature, pH and ozone concentration [2]. Ozone reacts with organic compounds dissolved in water through either direct ozone attack or indirect free radical attack. The hydroxyl radicals are generated by ozone disintegration in aqueous solutions [2]. During the ozonation process, dyestuffs lose their color by the oxidative cleavage of the chromophores. The cleavage of carbon–carbon double bonds and other functional groups, which have high electron densities, will shift the absorption spectra of the molecule out of the visible region [3].

Various types of dyes are used in many industries, such as paint, textile, plastics, ink, and cosmetics. A large amount of them is lost in the process of their manufacturing and utilization and causes environmental problems. Dyestuffs regulation on the discharge of dye-polluted colored wastewater has been getting stringent in many countries. Of all chemically synthesized dyestuffs, azo dyes are produced in the largest quantities. The treatment of dyes by activated sludge is ineffective. Generally, adsorption on activated carbon and coagulation by a chemical agent are applied to such effluents [4]. But these methods used

* Corresponding author. Tel.: +90 442 231 4601.
E-mail address: eoguz@atauni.edu.tr (E. Oguz).

1385-8947/$ – see front matter © 2007 Elsevier B.V. All rights reserved.
doi:10.1016/j.cej.2007.11.002

in the treatment processes merely transfer dye from water into solid and, thus further treatment process is necessary for the ultimate solution.

The disposal of dye wastewater is an environmental concern since the associated color is quite noticeable to the public, and some azo dyes may have carcinogenic and teratogenic effects on public health. Investigators have reported that conventional treatment processes do not readily remove dyes from textile wastewater, because of their stability to light, and biological degradation [5].

Although some treatment processes, such as chemical coagulation and carbon adsorption, may remove certain amount of dyestuffs to about 90% [6], the main drawback of these processes is the generation of a large amount of sludge waste, resulting in high operational costs for sludge treatment and disposal. An affordable and easy-operated control technology without the formation of sludge is needed to comply with today's demanding legislation. One choice is advanced chemical oxidation. The use of chlorinated oxidants, such as chloramine and chlorine dioxide, is not suggested since toxic or less biodegradable chlorinated by-products may be formed [7].

The main problem in the treatment of textile dying wastewater and dye manufacture wastewater is the removal of dye color [8]. In the late 1950s, the trickling filters and activated sludge processes were shown to be capable of removing the color of 84–93% in textile effluents. However, the color of wastewater from today's new dyes is difficult enough to treat by physical techniques, chemical processes and adsorption to achieve complete decolorization, especially for highly soluble dyes. Apart from the physical methods of decolorization, chemical oxidation using oxidants such as ozone, chlorine or hypochlorite, hydrogen peroxide, potassium permanganate can be used to destroy the dye to a colorless solution. The breakdown products can be removed by conventional biological treatment processes [9]. As one of the common oxidation agent, ozone has been applied to many fields in water and wastewater treatment and is considered as one of the potential methods for a combined treatment of effluents from textile dyeing and finishing industry.

Activated carbon has a lot of many applications, one of which is used as an efficient and versatile adsorbent for purification of water, air and many chemical and natural products [10]. This is possible due to the highly porous nature of the solid and its extremely large surface area to volume ratio. Much of this surface area is contained in micropores and mesopores. Currently, activated carbon has been an effective adsorbent for dye removal [11–15]. The adsorption capacity of a certain carbon is known to be a function of porous structure, chemical nature of the surface, and pH of the aqueous solution. In addition, the adsorption process is influenced by the nature of the adsorbate and its substituent groups [16].

The main objective of this work is to study the degradation kinetics of the 1:2 metal complex dyestuffs and to define the apparent rate constants by ozonation under the different experimental conditions, such as dye concentrations (400–1000 ppm), ozone–air flow rates (5–15 l min^{-1}), the percentage of O_3 in the ozone–air flow rate (0.7–1.4), pH (3–12), temperatures (18–70 °C), powder activated carbon (PAC) (0.5–1.5 g in solution of 250 ml), HCO_3^- (0–26 mM) and H_2O_2 concentrations (0–21 mM). In addition to the apparent rate constants, the modeling of artificial neural network (ANN) was used to predict the concentrations of dyestuffs removed from aqueous solution during ozonation under the different conditions. A relationship between the predicted results of the designed ANN model and experimental data was also conducted. In the result of this study, the determination coefficient (R^2), standard deviation ratio, mean absolute error and root mean square error in the modeling of ANN were defined as 0.978, 0.146, 19.503 and 56.600, respectively.

2. Materials and methods

2.1. Preparation of 1:2 metal complex dyestuffs

1:2 metal complex dyestuffs were used to prepare the dye solutions of 400, 600, 800 and 1000 mg l^{-1} of which the values of original pH are 9.3.

2.2. Preparation of H_2O_2 and HCO_3^- solutions

7, 14 and 21 mM hydrogen peroxide and 6, 13 and 26 mM HCO_3^- solutions were prepared from hydrogen peroxide (50% solution, 1.2 g/ml) and $NaHCO_3$ (Merck), respectively.

The reason for the use of hydrogen peroxide is to increase the $OH^\bullet$ radicals in O_3/H_2O_2 process because the oxidation potential of hydroxyl radicals is much higher than that of the ozone molecules. Thus, the increase of $OH^\bullet$ radicals in O_3/H_2O_2 process showed a positive enhancement in the apparent rate constants.

HCO_3^- ions in the O_3/HCO_3^- process were used to scavenge occurring $OH^\bullet$ radicals during ozonation. It is likely that bicarbonate is the principal consumer of the hydroxyl radicals, particularly when relatively high concentrations of bicarbonate are present in water. The scavenging effect of bicarbonate also lies in the fact that it reacts with hydroxyl radicals to generate bicarbonate radicals ($HCO_3^{\bullet -}$). These act as a very selective additional oxidation species and bicarbonate radicals have a much lower reaction rate constant than hydroxyl radicals for the oxidation of organic micropollutants [17].

2.3. Analytical methods

It was defined that 1:2 metal complex dyestuffs gave a peak at 505 nm. Dye removal capacity was determined by absorbance measurements at the maximum visible absorbance wavelength of 505 nm. All the samples to measure dye concentrations were analysed at 505 nm [18–21].

Bomaplex Red CR-L dye used in this study is a basic dye and the chemical structure of this water-soluble dye is given in Fig. 1.

In the O_3/PAC process, a commercial activated carbon from Merck was used as the adsorbent and its surface area was 455 m^2/g [19–21].

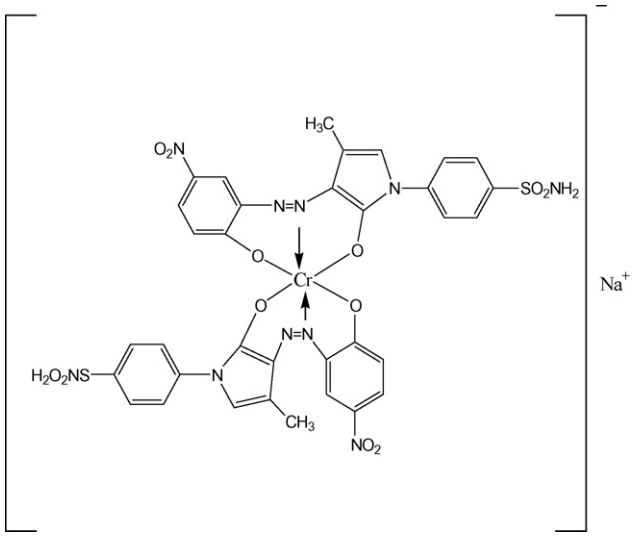

Fig. 1. The general chemical structure of the Bomaplex Red CR-L group dyes.

2.4. Ozonation studies

The ozonation reactor has been built by a glass column of 7-cm diameter, 40-cm height with a water-cooling jacket keeping the reactor at constant temperature. Two hundred and fifty millilitres of solution was used for each batch ozonation. A magnetic stirrer was used with the gas diffuser for sufficient circulation of the dye solution. 1:2 metal complex dyestuffs used in this study were supplied from a textile mill in Turkey (Dye textile industry company project, Gaziantep) [18–21]. The experimental set-up shown in Fig. 2 includes an air dryer, compressor, ozone generator and semi-batch reactor having 1 l of volume. Ozone was generated using an ozonizer Model OG–24 [18–21].

Ozone was generated from air, and was supplied into the system through an Opal OG-24 model ozonizer at the rates of 5, 10 and 15 l min^{-1}. The ozonation was performed in a cylindric semi-batch glass reactor (volume 1 l). 1:2 metal complex dyestuffs were ozonated for 20 min in the semi-batch reactor. The ozone–air mixture percentages (0.7, 1.1 and 1.4 O_3%) were continuously sparged through a diffuser in the solution [18–21].

2.5. ANN software

In order to model the removal of dyestuffs with ANN, the Statistica 6 software program was used.

3. Results

3.1. Determination of the apparent rate constants of dyestuffs by ozonation

The ozonation of 1:2 metal complex dyestuffs was considered as a second-order reaction with first-order relative to the dyestuffs [C] and ozone [O_3] concentrations. The rate of 1:2 metal complex dyestuffs disappearance could be formulated by Eq. (1)

$$V = -\frac{dC}{dt} = k[O_3][C] \quad (1)$$

where k is the second-order rate constant. When the amount of ozone is in excess, the reaction is pseudo-first-order with respect to the dyestuffs. In this study, the pseudo-first-order trend was observed in each of the experimental runs. Hence, ozone concentration could be considered constant during reaction and the expression of the rate of 1:2 metal complex dyestuffs degradation was given by Eq. (2).

$$V = -\frac{dC}{dt} = k'[C] \quad (2)$$

where k' is apparent first-order kinetic constant (min^{-1}). Therefore, a plot of $\ln[C_o/C]$ versus the reaction time led to a straight line from which k' could be determined. The apparent rate constant of reaction was calculated from Eq. (3).

$$k' = k[O_3] \quad (3)$$

where [O_3] is the ozone concentration (ozone saturation concentration).

The kinetics of removal of dyestuffs from the synthetic aqueous solutions were investigated under the different experimental conditions (C_o: 400, 600, 800 and 1000 mg/l; Q: 5, 10 and 15 l min^{-1}; T: 18, 40 and 70 °C; O_3: 0.7, 1.1 and 1.4%; pH: 3, 6, 9.3 and 12; HCO_3^-: 0, 6, 13 and 26 mM; H_2O_2: 0, 7, 14 and 21 mM; PAC: 0, 0.5, 1 and 1.5 g). The results of this study which were realized at various experimental conditions are shown in Figs. 3–10. At different empirical conditions, the experimental results of dyestuffs ozonation showed that the ozonation reaction kinetics followed a pseudo-first-order reaction ($R^2 \approx 1$).

Fig. 3 shows the change of $\ln(C_o/C)$ and the apparent rate constants versus time and the concentration of dyestuffs, respectively. As seen in Fig. 3, the apparent rate constants do not change

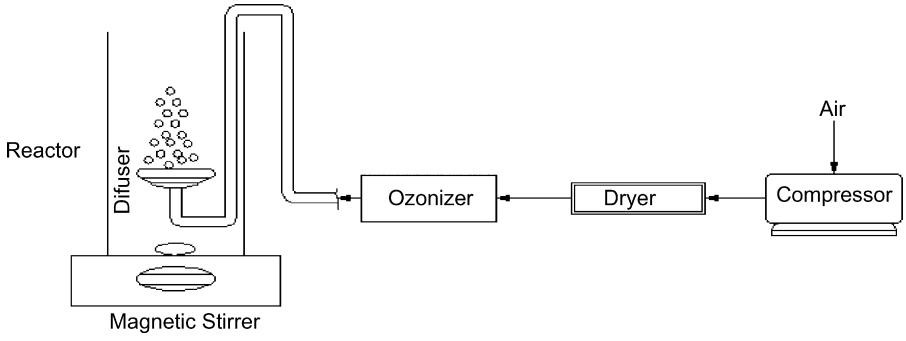

Fig. 2. Ozonation system used in the oxidation.

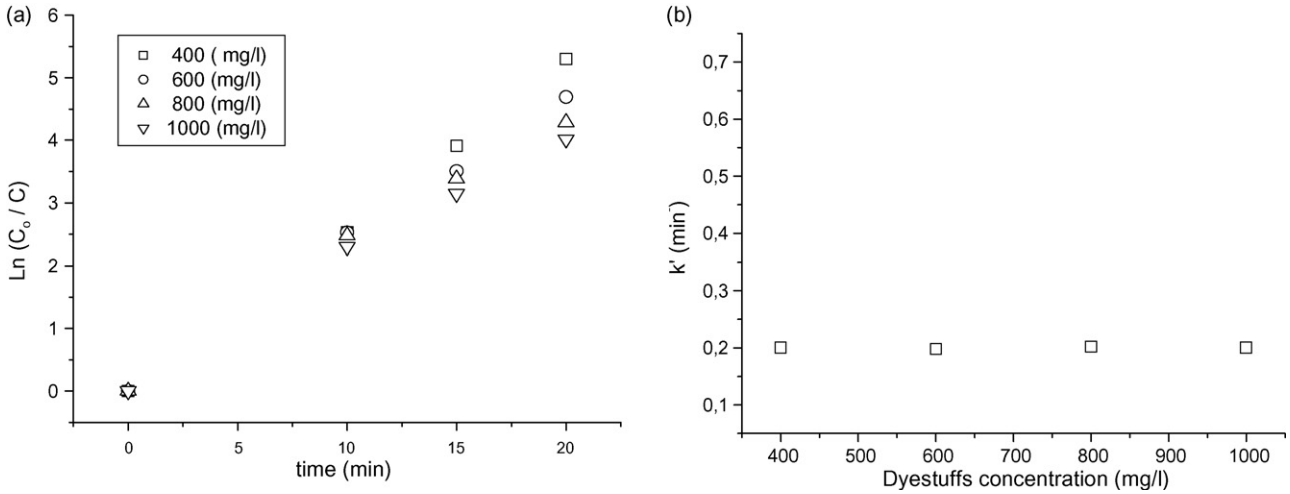

Fig. 3. (a) The plot of $\ln(C_o/C)$ vs. time, (b) the plot of apparent rate constants vs. dyestuffs concentration (T: 18 °C, Q: 5 l min^{-1}, O_3: 1.4%, pH: 9.3, HCO_3^-: 0 mM, H_2O_2: 0 mM, PAC: 0 g).

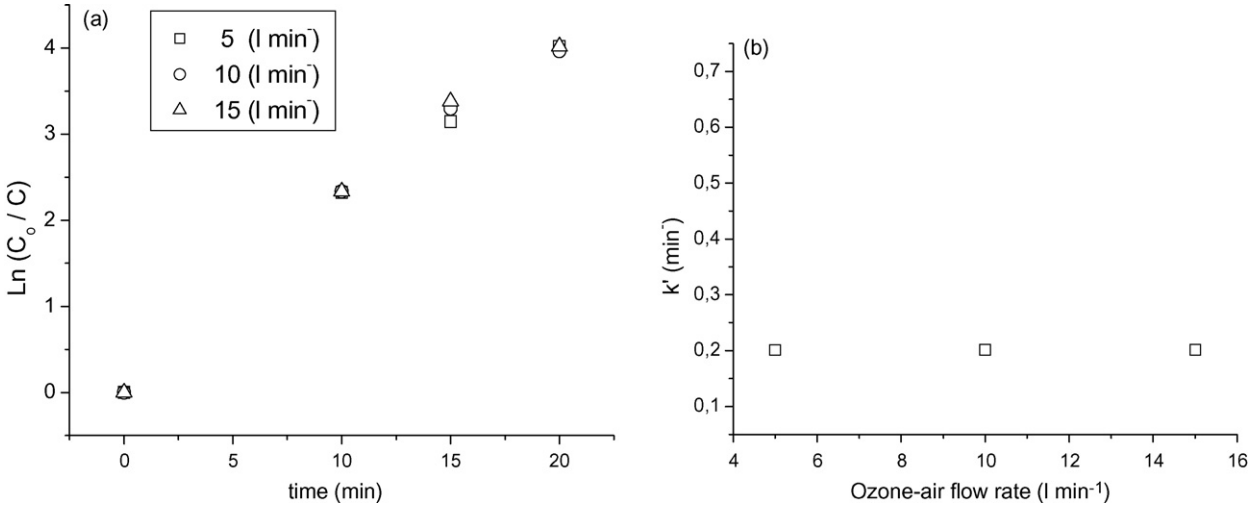

Fig. 4. (a) The plot of $\ln(C_o/C)$ vs. time, (b) the plot of apparent rate constants vs. ozone–air flow rate (C_o: 1000 mg/l, T: 18 °C, O_3: 1.4%, pH: 9.3, HCO_3^-: 0 mM, H_2O_2: 0 mM, PAC: 0 g).

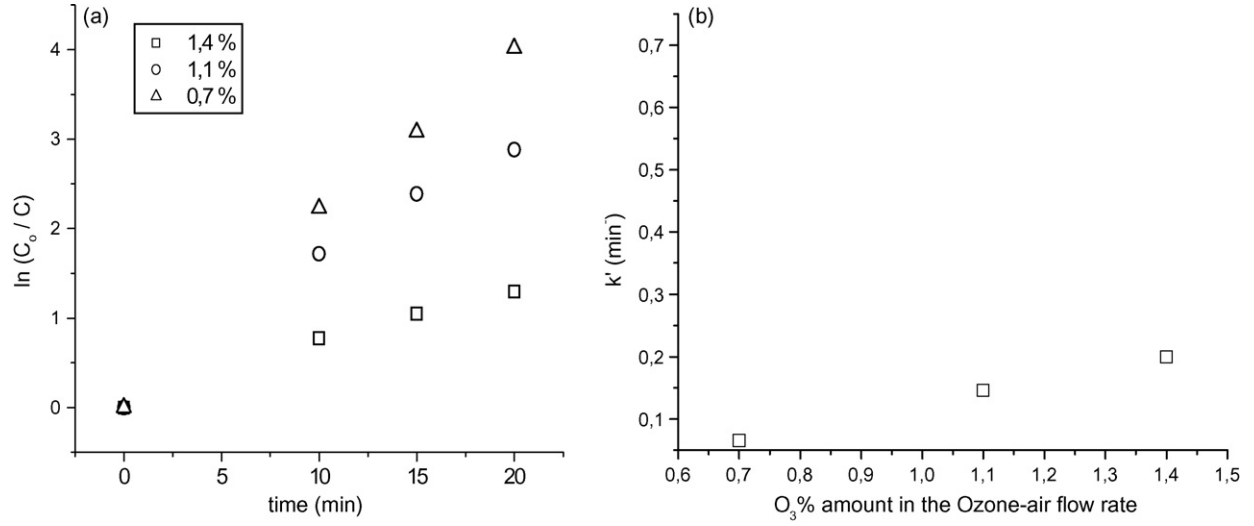

Fig. 5. (a) The plot of $\ln(C_o/C)$ vs. time, (b) the plot of apparent rate constants vs. O_3% amount (C_o: 1000 mg/l, T: 18 °C, Q: 5 l min^{-1}, pH: 9.3, HCO_3^-: 0 mM, H_2O_2: 0 mM, PAC: 0 g).

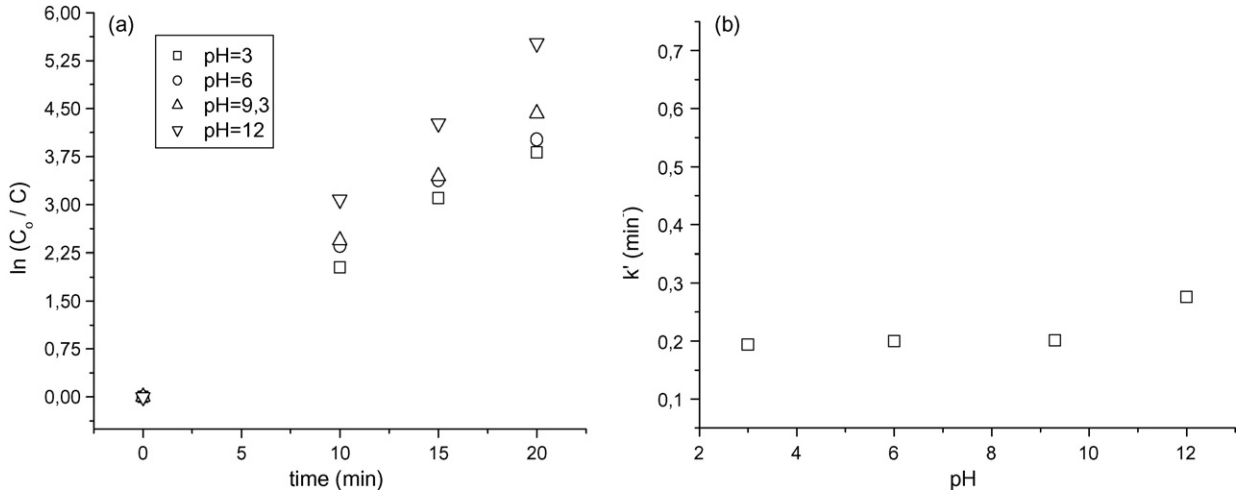

Fig. 6. (a) The plot of $\ln(C_o/C)$ vs. time, (b) the plot of apparent rate constants vs. the value of pH (C_o: 1000 mg/l, T: 18 °C, Q: 5 l min^{-1}, O_3: 1.4%, HCO_3^-: 0 mM, H_2O_2: 0 mM, PAC: 0 g).

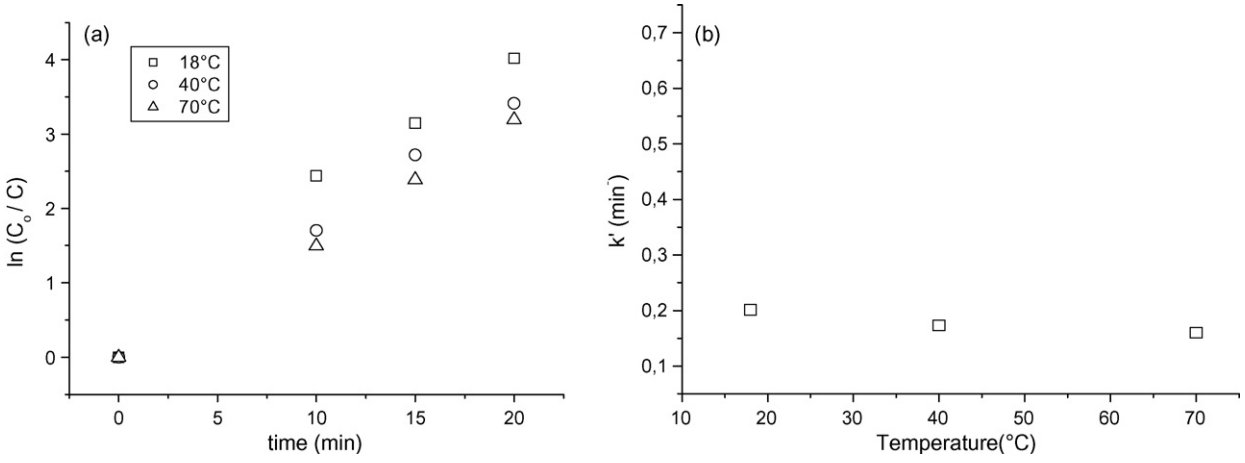

Fig. 7. (a) The plot of $\ln(C_o/C)$ vs. time, (b) the plot of apparent rate constants vs. the temperature of solution (C_o: 1000 mg/l, pH: 9.3, Q: 5 l min^{-1}, O_3: 1.4%, HCO_3^-: 0 mM, H_2O_2: 0 mM, PAC: 0 g).

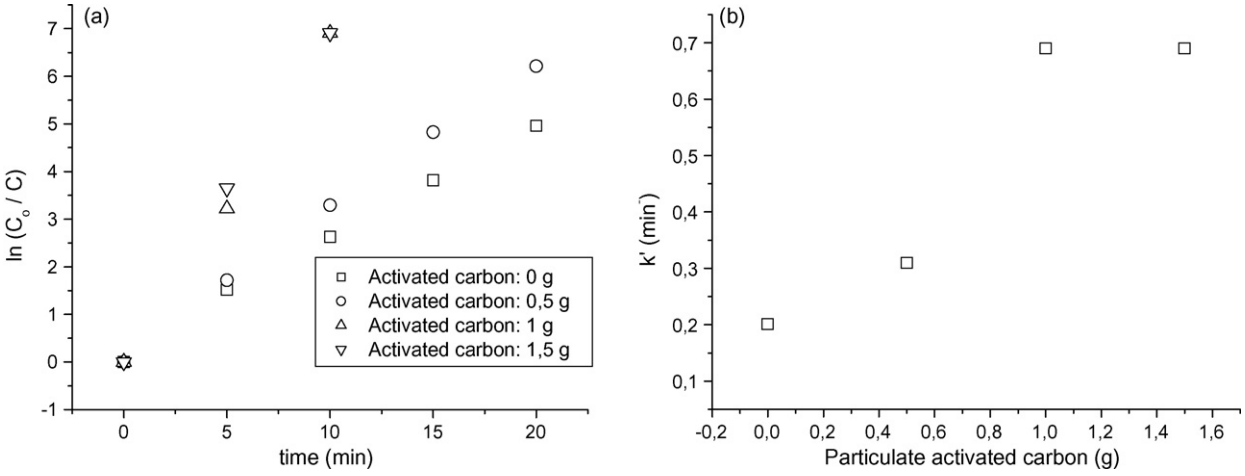

Fig. 8. (a) The plot of $\ln(C_o/C)$ vs. time, (b) the plot of apparent rate constants vs. the PAC dosages used in the solution (C_o: 1000 mg/l, pH: 9.3, Q: 5 l min^{-1}, O_3: 1.4%, HCO_3^-: 0 mM, H_2O_2: 0 mM).

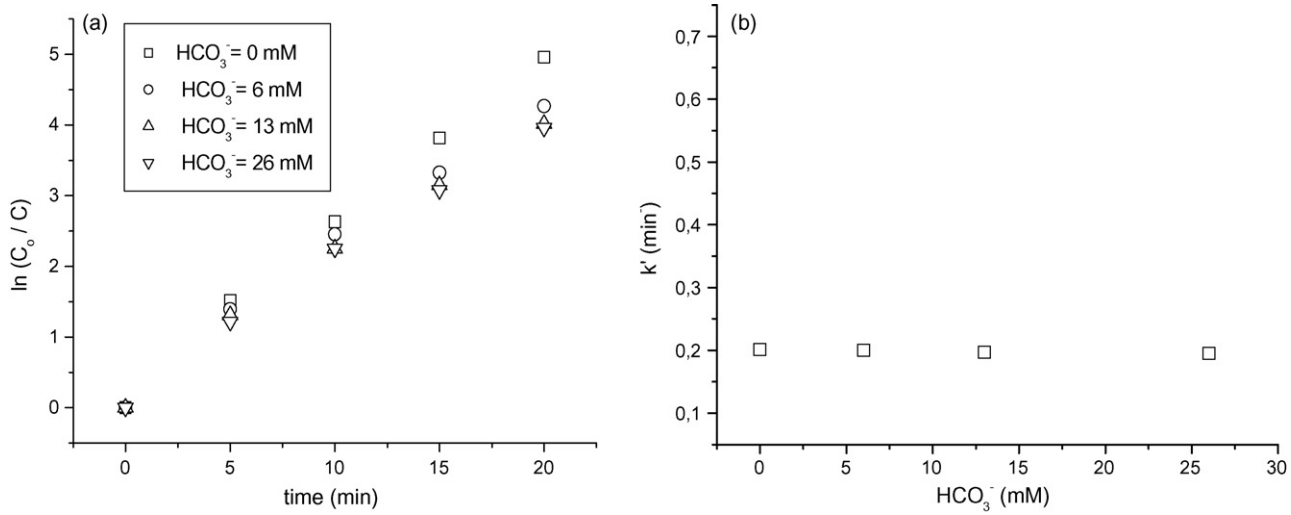

Fig. 9. (a) The plot of $\ln(C_o/C)$ vs. time, (b) the plot of apparent rate constants vs. the HCO_3^- ion concentration (C_o: 1000 mg/l, pH: 9.3, Q: 5 l min^{-1}, O_3: 1.4%, H_2O_2: 0 mM, PAC: 0 g).

with increase of dyestuffs concentration. It was thought that unimportant changes in the apparent rate constants arose from empirical errors, but as seen from Fig. 3, these errors are not significantly meaningful.

As seen in Fig. 4, the apparent rate constants in the dyestuffs removal increased with the increase of ozone–air flow rate from 5 to 10 l min^{-1}, but the value of apparent rate constant at 15 l min^{-1} did not change and this value was approximately the same that at 10 l min^{-1}. It was though that the reason for the apparent rate constants at 10 and 15 l min^{-1} did not change is due to the fact that the ozone–air flow rate at 15 l min^{-1} was in large excess, and some of the ozone–air mixture left from solution without dissolution.

Fig. 5 shows the change in apparent rate constants with the increase of ozone generation percentages (from 0.7 to 1.4 O_3%). The apparent rate constants increased with the augmentation of ozone generation percentage. It was thought that the more double bonds in molecular O_2 were broken with the increase of ozone generation percentage, the more molecules of O_3 occurred. O_3 molecules attracted to the double bonds in the dye molecules, and these bonds were broken by ozone. With more dye molecule degradation, more dye molecules were removed from aqueous solution, and thus the apparent rate constant at the value of 1.4 O_3% was max as seen from Fig. 5.

At various initial pH values (3, 6, 9.3 and 12), the change of apparent rate constants of 1:2 metal complex dyestuffs by ozonation was investigated, and it was shown in Fig. 6. The apparent rate constants of 1:2 metal complex dyestuffs were found to have increased with the augmentation of pH during ozonation time. As known, ozone oxidation pathways include direct oxidation by ozone or radical oxidation by $OH^\bullet$ radical. Direct oxidation with ozone is more selective and predominates under acidic conditions, while radical oxidation with $OH^\bullet$ radical is less selective and predominates under basic conditions. Since the oxidation

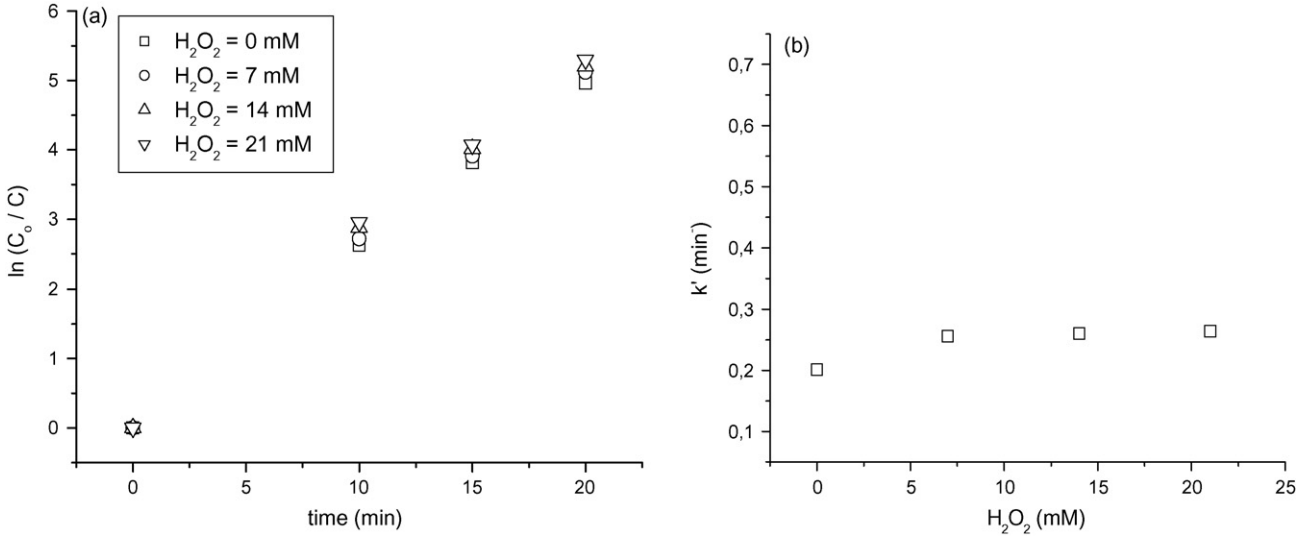

Fig. 10. (a) The plot of $\ln(C_o/C)$ vs. time, (b) the plot of apparent rate constants vs. the H_2O_2 concentration in the solution (C_o: 1000 mg/l, pH: 9.3, Q: 5 l min^{-1}, O_3: 1.4%, HCO_3^-: 0 mM, PAC: 0 g).

potential of hydroxyl radicals is 2.08 V and much higher than that of the ozone molecule (1.86 V), direct oxidation is slower than radical one. During an ozonation of 20 min, the increase in the solution pH showed a positive enhancement on the ozone oxidation of 1:2 metal complex dyestuffs. The ozonation of the dyestuffs at the various initial pH values (3, 6, 9.3 and 12) was examined, and it was observed that the values of apparent rate constants increased with the augmentation of pH as seen from Fig. 6.

Ozone disintegration in aqueous solutions generates hydroxyl radicals. At higher pH, ozone reacts with hydroxide ions, and then forms hydroxyl radicals. Due to fact that the oxidation rate increases with the augmentation of pH values, the pH of solution directly affects the mechanism of oxidation. Thus, the value of k' increases at the values of pH higher than 9.

As seen from Fig. 7, as a result of the ozonation of the dyestuffs, the values of the apparent rate constants decreased with the increase of temperature from 18 to 70 °C. After a 20 min ozonation, the highest value of apparent rate constant connected with temperature was received at 18 °C. It was thought that the decrease of ozone solubility in the solution with the increase of temperature caused the decrease in the values of apparent rate constants.

At the different PAC dosages such as 0, 0.5, 1 and 1.5 g in the solution of 250 ml, the values of apparent rate constants of dyestuffs by ozonation are shown in Fig. 8. The values of apparent rate constants of dyestuffs by ozonation increased with the augmentation of PAC dosage from 0 to 1 g, but remained unchanged from 1 to 1.5 g. In the present study, it was thought that PAC played an important role as adsorbent. The PAC used to remove dyestuffs from synthetic aqueous solution has quite a positive effect on the treatment of dyestuffs wastewater. As is known, the ozone dissolved in the solution is consumed by PAC particles. Two mechanisms are involved in the oxidation of carbon black by ozone: (i) direct oxidation of elemental carbon to CO_2; and (ii) oxidation of elemental carbon to intermediate and subsequently oxidation to CO_2 [22,23]. Because of these mechanisms, it was thought that PAC particles of 1.5 g which were too much in the solution partly prevented ozone molecules to react with the dyestuffs molecules and the PAC particles consumed dissolved ozone concentration in the solution. Because of these reasons, at the level of PAC of 1.5 g, the value of apparent rate constant of dyestuffs by ozonation did not change as seen from Fig. 8.

Fig. 9 shows the value of apparent rate constants in the O_3/HCO_3^- process. HCO_3^- ions in the O_3/HCO_3^- process scavenge the produced from ozonation $OH^\bullet$ radicals. Bicarbonate ions are the principal consumer of the hydroxyl radicals, particularly when relatively high concentrations of bicarbonate are present in water. HCO_3^- ions react with hydroxyl radicals to generate bicarbonate radicals ($HCO_3^{\bullet -}$) [24]. It was reported that bicarbonate ions scavenged hydroxyl radicals to produce intermediates, not releasing a radical-type chain carrier, thereby quenching the radical type chain reaction [24]. Because of the scavenging effect of bicarbonate ions on the $OH^\bullet$ radicals, the value of apparent rate constants of dyestuffs ozonation decreased with the increase of HCO_3^- ion concentration. When HCO_3^- ions were not used in the aqueous solution, the value of apparent rate constant received a max value as seen from Fig. 9.

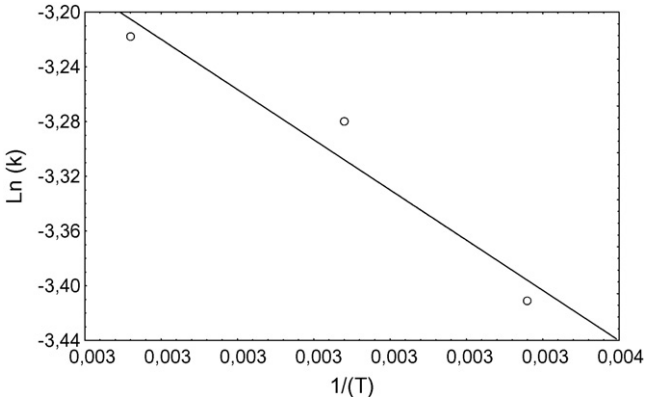

Fig. 11. The plot of ln(k) vs. (1/T).

Since the oxidation potential of hydroxyl radicals is much higher than that of the ozone, direct oxidation by ozone is slower than radical one. The increase of $OH^\bullet$ radicals in the solution showed a positive enhancement in the apparent rate constants, and the value of apparent rate constant in the H_2O_2/O_3 process increased with the augmentation of H_2O_2 concentration in the solution as depicted in Fig. 10.

Arrhenius equation used to define the value of activation energy (E_a) is given by the Eq. (4)

$$\ln k = \ln A - \frac{E_a}{R}\frac{1}{T} \tag{4}$$

where k, A, E_a, R and T, reaction rate constant, pre-exponential factor, activation energy (J mol^{-1}), ideal gas constant (8,314 J mol^{-1} K^{-1}) and temperature (K), respectively. A plot of ln k versus 1/T would result in a straight line with a slope of ($-E_a/R$) and intercept of ln A as seen in Fig. 11.

The value of E_a calculated using the Arrhenius equation was found as 3 kJ mol^{-1} which was smaller than the value of 20 kJ mol^{-1}. Thus, the reaction of ozonation of dyestuffs under the different temperatures such as 291, 313 and 343 K was defined as diffusion control.

3.2. Application of artificial neural network (ANN)

The linear model presents the disadvantage to give a relationship very satisfying for an oxidation study, subject to the real independence of variables. In fact, it is reasonable to consider that such variables are not exactly independent. ANN approach seems to be completely suitable to the problems where the relations between variables are not linear and complex [25].

ANNs are direct inspiration from the biology of human brain, where billions of neurons are interconnected to process a variety of complex information, accordingly, a computational neural network consists of simple processing units called neurons. Each neuron (a processing element) is linked to its neighbors with varying strengths, the strength of connection between two neurons is called *weight* and is represented by coefficients of connectivity w. The architecture of ANNs used in this study is shown in Fig. 12.

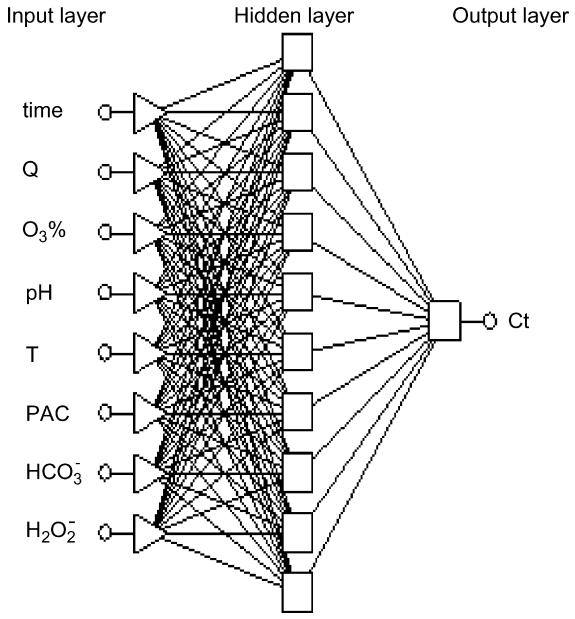

Fig. 12. The architecture of the ANNs used in this study.

As shown in Fig. 12, a neural net is parallel interconnected structure consisting of: (1) input layer of neuron (independent variables); (2) a number of hidden layers; and (3) output layer (dependent variables). The number of input and output neurons is determined by the nature of the problem. The hidden layers act like feature detectors and in theory, there can be more than one hidden layer. Universal approximation theory suggests that a network with a single hidden layer with a sufficiently large number of neurons can interpret any input–output structure [26]. Input neurons accept the input data characterizing a given observation (experiment), output neurons yield the predicted (expected) value. A neuron sums the product of each connection weight (w_{jk}) from a neuron (j) to the neuron (k) and input (x_j) and the additional weight called as the bias to get the value of sum for the neuron (k):

$$\text{sum}\, k = \sum w_{jk} x_j + bias_k$$

The sum of the weighted inputs is further transformed with a *transfer function* to get the output value, and there are several transfer functions; the most common is the sigmoidal function [27].

There are a lot of different training algorithms. Some of these are back propagation, conjugate gradient descent, quasi-Newton, quick propagation and Levenberg–Marquardt. A popular algorithm is the back propagation, which has different variants. Back propagation training algorithms that employ gradient descent and gradient descent with momentum are often too slow for practical problems because they require small learning rates for stable learning. This algorithm has problem in converging properties. In addition, the success in the algorithm depends on the user-dependent parameters, learning rate and momentum constant [28].

The Levenberg–Marquardt algorithm yielded best results in this study. This algorithm is a variation of Newton's method which is designed for minimizing functions that are sums of square of other nonlinear functions. This is very well suited to neural network training where the performance index is the mean squared error. Levenberg–Marquardt algorithm is shown in Eq. (5) [29].

$$x_{k+1} = x_k - [J^T(x_k)J(x_k) + \mu_k I]^{-1} J^T(x_k)\upsilon(x_k) \quad (5)$$

where J, μ_k, I, x_k are Jacobian matrix, Marquardt parameter, unit matrix and iteration k, respectively. This algorithm has the very useful feature that as μ_k is increased it approaches the steepest descent algorithm. As μ_k is decreased to zero the algorithm becomes Gauss–Newton.

In this study, one-layered back propagation neural network was used for modeling of the removal of dyestuffs with ozonation (Fig. 12). The input variables to the neural network are as follows: the treatment time (t), the initial concentration of H_2O_2, temperature, PAC, ozone–air flow rate, the percentages of O_3 in the ozone–air flow rate, pH and HCO_3^- ion concentration. The concentration of removal of dyestuffs, as a function of reaction time, was chosen as the experimental response or output variable.

Before the training of the network, both input and output variables were normalized within the range 0–1 using minimax algorithm. The minimum and maximum of the data set were found and scaling factors were selected so that these were mapped to desired minimum and maximum values. The minimax algorithm is given by Eq. (6)

$$H' = H \underbrace{\left\{\frac{1}{H_{\text{MAX}} - H_{\text{MIN}}}\right\}}_{\text{scale factor}} - \underbrace{\left\{\frac{H_{\text{MIN}}}{H_{\text{MAX}} - H_{\text{MIN}}}\right\}}_{\text{shift factor}} \quad (6)$$

where $H_{\max}$ and $H_{\min}$, respectively indicate the largest and smallest values of H, and H' the unified value of the corresponding H. Normalization of the data greatly improves learning speed and it is beneficial in reducing the error of the trained network.

Of the 203 experimental data sets were divided into three sections: the training set (143 data), verification set (30 data) and test set (30 data). Training algorithms do not use the verification or test sets to adjust network weights. The verification set may optionally be used to track the network's error performance, to identify the best network and to stop training if over-learning occurs. The test set is not used in training at all, and it is designed to give an independent assessment of the network's performance when an entire network design procedure is completed. Seventy percent of the data set was used to train the network, while the remaining 30% was employed for testing and verification. The assignment of cases to the training, verification and test subsets can sometimes affect the performance of training algorithms. In order to eliminate this situation, the cases should be shuffled randomly between subsets. The cases can be left in their original order, or grouped together in the subsets. In this model, the cases were shuffled randomly between subsets (training, test and verification).

In order to model the dyestuffs concentrations with ANNs, the Statistica software program was used. The coefficient of determination (R^2), the root mean square error (RMSE), the standard deviation ratio (SDR), and the mean absolute error (MAE) are

the main criteria that are used to evaluate the performance of ANN, and they are defined as follows [30,31]:

$$R = \frac{n\left(\sum \text{observed} - \text{predicted}\right) - \left(\sum \text{observed}\right)\left(\sum \text{predicted}\right)}{\sqrt{\left[n\sum \text{observed}^2 - \left(\sum \text{observed}\right)^2\right]\left[n\sum \text{predicted}^2 - \left(\sum \text{predicted}\right)^2\right]}} \quad (7)$$

$$\text{RMSE} = \sqrt{\frac{(\text{observed} - \text{predicted})^2}{n}} \quad (8)$$

$$\text{SDR} = \frac{\sqrt{n\sum \text{observed}^2 - \left(\sum \text{observed}\right)^2/n(n-1)}}{\sqrt{n\sum \text{error}^2 - \left(\sum \text{error}\right)^2/n(n-1)}} \quad (9)$$

$$\text{MAE} = \frac{\sum |\text{observed} - \text{predicted}|}{n} \quad (10)$$

Before the network was trained, the input and the output data had been normalized, and the scale and shift factors which were used in every input and output were given in Table 1.

After long training phases, the best result was obtained from the Levenberg–Marquardt algorithm. The hyperbolic tangent function in the hidden layer and the linear activation function in the output layer were used in the model. It was observed that optimal network was found to be eight inputs; one hidden layer with ten neurons and one output layer, the optimal network architecture ($8 \times 10 \times 1$) is shown in Fig. 12.

Statistica Neural Networks can conduct a sensitivity analysis on the inputs to a neural network. This indicates which input variables are considered most important by that particular neural network. There are also facilities to prune out input variables with low sensitivity. Sensitivity analysis can give important insights into the usefulness of individual variables. It often identifies variables that can be safely ignored in subsequent analysis, and key variables that must always be retained. Input variables are removed from the network that has low sensitivity (i.e. that have no significant effect on the accuracy of the network). Units with both training and verification ratios below the threshold are removed. A ratio of 1.0 indicates that the variable has no positive effect on the model at all, and can definitely be removed. A ratio below 1.0 indicates that the model actually performs better if the variable is removed. The results of the sensitivity analysis were given in Table 2.

When Table 2 is examined, it is easy to see that the most important parameters that affect the removal of concentration of dyestuffs are the treatment time (t), temperature (T), O_3%, Q, PAC, HCO_3^-, pH, and H_2O_2, respectively. It the result of in this study, the general equation obtained from the optimal network was given as follows:

$$C_t = f_2\left(w_2 f_1\left(w_1\begin{bmatrix} t \\ Q \\ O_3 \\ \text{pH} \\ T \\ \text{PAC} \\ HCO_3^- \\ H_2O_2 \end{bmatrix} + b_1\right) + b_2\right) \quad (11)$$

where w_1 and w_2 are the weight matrices, b_1 and b_2 are the biases vectors. Under the different experimental conditions along the reaction time, the interpretation of the experimental results was based on the fitting of neural network models for predicting the removal of concentration of dyestuffs by ozonation. The proposed model based on artificial neural network (ANN) could predict the dyestuffs concentration during ozonation time. A comparison between the predicted results of the designed ANN model and experimental data was also conducted.

According to the ANN model fundamentals, with use of more data for training the network, better result would be obtained. In the early standard algorithm, random initial set of weights were assigned to the neural network, and then by considering the input data, weights were adjusted, and thus the output error would be on its minimum. The results from general ANN modeling were shown in Fig. 13. Four data in Fig. 13 were outliers but it was thought that these data which were outliers would not affect the performance of general model.

The general model from the ANN belonging to all of the parameters (ozone–air flow rates, O_3% amounts in the ozone–air flow rate, pHs, temperatures, PAC, HCO_3^- and H_2O_2 concentrations) was given in Fig. 13.

Table 1
Shift and scale factors

Parameters	Shift	Scale
t (treatment time) (min)	0	0.033
Q (ozone–air flow rates) ($l\,min^{-1}$)	−0.500	0.100
O_3 (O_3 amounts in the ozone–air flow rate) (%)	−1	1.428
pH	−0.333	0.111
T (temperature) (°C)	−0.346	0.019
PAC (powder activated carbon) (g)	0	0.666
HCO_3^- (hydrogen peroxide mM) (mM)	0	0.038
H_2O_2 (bicarbonate) (mM)	0	0.047
C_t (the dyestuffs concentration at time t) (ppm)	0	0.001

Table 2
Sensitivity analysis results

	t	Q	O_3%	pH	T	PAC	HCO_3^-	H_2O_2
Ratio	7.548	1.516	2.484	1.204	2.572	1.499	1.373	1.083
Rank	1	4	3	7	2	5	6	8

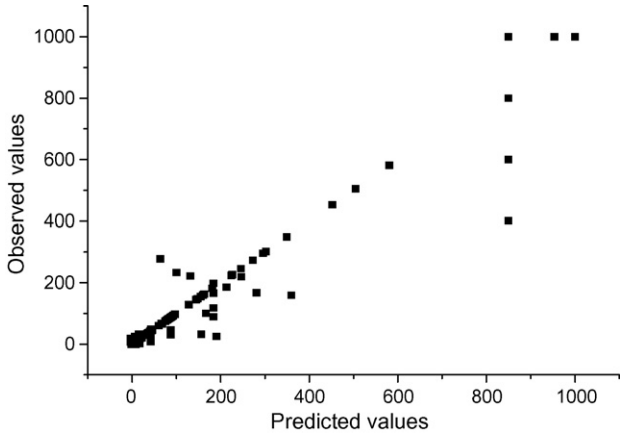

Fig. 13. Comparison between observed and predicted values relating to general modeling ($R^2 = 0.978$).

Table 3
The statistical values of ANN model (8 × 10 × 1)

R^2	0.978
SDR	0.146
RMSE	56.600
MAE	19.503

The results of statistical analysis of ANN were summarised in Table 3. It was seen that the ANN model had determination coefficient of (0.978), SDR of (0.146), RMSE of (56.600) and MAE of (19.503). The results obtained in this model indicate that ANN model has the ability to predict the removal of concentration of dyestuffs.

In the ANN modeling, it was seen that the error distributions of the model did not show complete normal distribution. Almost every value predicted in the model and the distribution of the errors are very close to the zero line as seen Fig. 14. Error distributions do not show complete normal distribution. It was also observed that almost every value predicted in the model and the distribution of the errors were not in the line of zero.

Every value predicted in the model and the distribution of the errors are very close to the zero line. The error histogram is

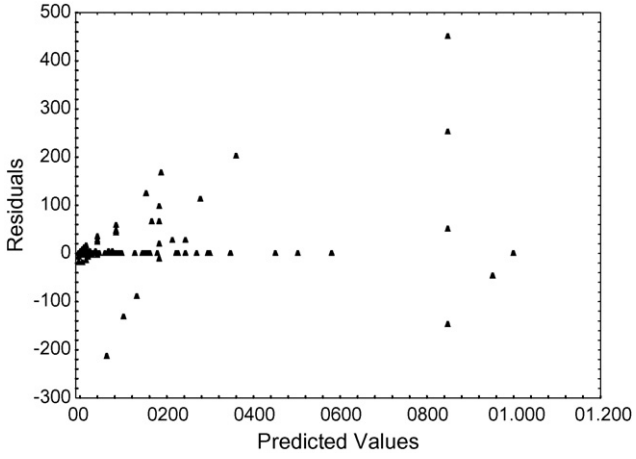

Fig. 14. Residuals vs. predicted values.

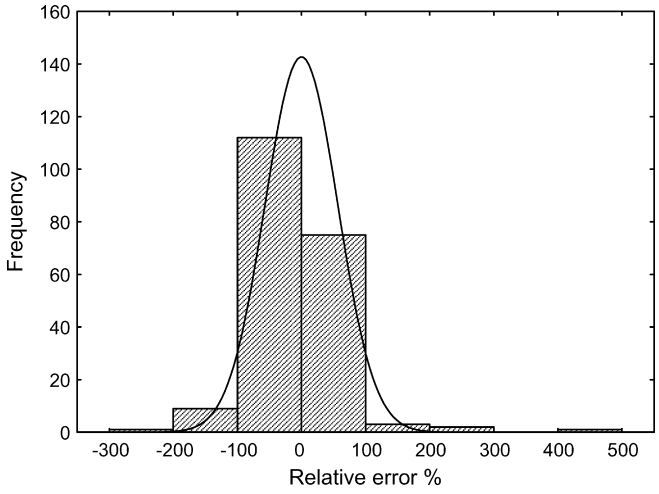

Fig. 15. Relative error distribution.

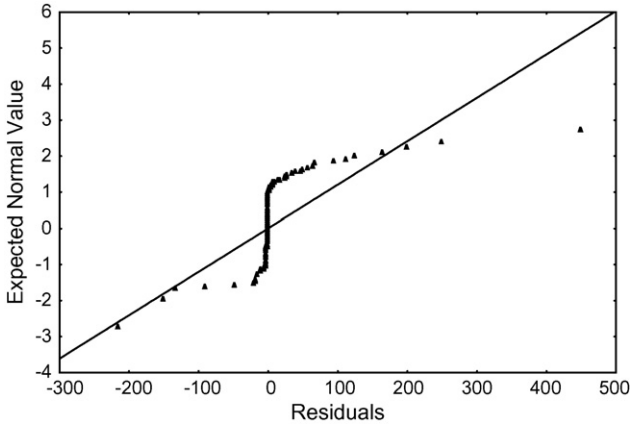

Fig. 16. Normal probability plot of residuals.

not widely open to the right and left directions. The zero error frequency is high and also in the model the predicted values together with the observed values are in good agreement as seen from Fig. 15. Moreover, the explanatory variables in the models to explain the dependent variable are found to be satisfactorily sufficient.

In a good model, the residuals show normal distribution. The assumption of normality can be checked by plotting the residual versus expected normal values. The normal probability plot of the residuals for ANN is shown in Fig. 16 which shows an approximately linear behavior, indicating that the residuals follow an approximately normal distribution.

4. Conclusion

This study demonstrated that dye degradation by ozonation under the different conditions tested fitted the pseudo-first-order reaction. The apparent degradation rate constants of 1:2 metal complex dyestuffs increased with the augmentation of ozone–air flow rate from 5 to 10 l min^{-1}, but it did not change from 10 to 15 l min^{-1}. At a high pH, the ozonation of dyestuffs contributed to the increase of the apparent rate constant because of occurring hydroxyl free radicals. The activation energy (E_a) of the reaction

was found 3 kJ mol^{-1} using Arrhenius equation. The reaction of ozonation of dyestuffs under the different temperatures (291, 313 and 343 K) was defined as diffusion-controlled because the value of E_a was smaller than 20 kJ mol^{-1}. Artificial neural network modeling was used to investigate the cause–effect relationship in the ozonation processes of dyestuffs. The ANN model could describe the behavior of the synergic reaction system (O_3/PAC, O_3/H_2O_2, O_3/HCO_3^- processes). Simulation based on the ANN model can then be performed in order to estimate the behavior of the system under different conditions. The model based on artificial neural network (ANN) could predict the concentrations of dyestuffs removal from aqueous solution during ozonation under the different conditions. A relationship between the predicted results of the designed ANN model and experimental data was also conducted. At the result of ANN model, the values of determination coefficient (R^2), standard deviation ratio, mean absolute error and root mean square error were obtained as 0.978, 0.146, 19.503 and 56.600, respectively.

References

[1] Y.S. Hung, Decolorization of mono-azo dyes in wastewater by advanced oxidation process: a case study of acid red 1 and acid yellow 23, Chemosphere 29 (1994) 2597–2607.

[2] B. Jurgen, Mixed results: latest study adds skepticism, hope to ozone debate, Textile Rental (February) (1995) 78–84.

[3] C. Nebel, Ozone decolorization of secondary dye-laden effluents, in: Second Symposium on Ozone Technology, Montreal, May 11–14, 1975, pp. 336–358.

[4] K. Higashi, M. Yamane, S. Takeda, A. Kawahara, S. Wakida, Research survey on prevention of pollution by wastewaters, Mizushorigijutsu 37 (1996) 187–200.

[5] G. Mishra, Critical review of the treatment for decolorization of textile effluent, Colourage 40 (1993) 35–38.

[6] C. Poon, B.M. Vittimberga, UV photo-decomposition of color in dyeing wastewater, in: Industrial Waste, Processing of 13th Mid-Atlantic Conference, 1981, pp. 427–433.

[7] M.L. Richardson, The aquatic environment and the mess made by metabolites, J. Soc. Dyers Colour. 99 (1983) 198–200.

[8] A.H. Konsova, Decolorization of wastewater containing direct dye by ozonation in a batch bubble column reactor, Desalination 158 (2003) 233–240.

[9] V. Rizzuti Augugu, O. Liar, G. Marrucci, Ozone absorption in alkaline solutions, Chem. Eng. Sci. 31 (1976) 877–880.

[10] J.W. Hassler, Activated Carbon, Chemical Publishing Company, Inc., NY, 1963.

[11] G.M. Walker, L.R. Weatherley, Textile wastewater treatment using granular activated carbon adsorption in fixed beds, Sep. Sci. Technol. 35 (2000) 1329.

[12] V. Meshko, L. Markovska, M. Mincheva, A.E. Rodrigues, Adsorption of basic dyes on granular activated carbon and natural zeolite, Water Res. 35 (17) (2001) 3357–3366.

[13] N. Kannan, M.M. Sundaram, Kinetics and mechanism of removal of methylene blue by adsorption on various carbons—a comparative study, Dyes Pigments 51 (2001) 25–40.

[14] W. Shaobin, Z.H. Zhu, C. Anthony, F. Haghseresht, G.Q. Lu, The physical and surface chemical characteristics of activated carbons and the adsorption of methylene blue from wastewater, J. Colloid Interface Sci. 284 (2005) 440–446.

[15] K.K.H. Choy, G. McKay, J.F. Porter, Sorption of acid dyes from effluents using activated carbon, Resour. Conserv. Recy. 27 (1999) 57–71.

[16] S. Yenisoy-Karakas, A. Aygun, M. Gunes, E. Tahtasakal, Physical and chemical characteristics of polymer-based spherical activated carbon and its ability to adsorb organics, Carbon 42 (2004) 477.

[17] J. Staehelin, J. Hoigne, Decomposition of ozone in water: rate of initiation by hydroxide ions and hydrogen peroxide, Environ. Sci. Technol. 16 (10) (1982) 676–681.

[18] E. Oguz, B. Keskinler, Z. Celik, Ozonation of aqueous bomaplex red CR-L dye in a semi-batch reactor, Dyes Pigments 64 (2005) 101–108.

[19] E. Oguz, B. Keskinler, Determination of adsorption capacity and thermodynamic parameters of the PAC used for bomaplex red CR-L dye removal, Colloids Surf. A 268 (2005) 124–130.

[20] E. Oguz, B. Keskinler, C. Celik, Z. Celik, Determination of the optimum conditions in the removal of bomaplex red CR-L dye from the textile wastewater using O_3, H_2O_2, HCO_3^- and PAC, J. Hazard. Mater. 131 (2006) 66–72.

[21] E. Oguz, B. Keskinler, Comparison among O_3, PAC adsorption, O_3/HCO_3^-, O_3/H_2O_2 and O_3/PAC processes for the removal of bomaplex red CR-L dye from aqueous solution, Dyes Pigments 74 (2007) 329–334.

[22] V.R. Deitz, J.L. Bitner, The reaction of ozone with adsorbent charcoals, Carbon 10 (1972) 145–154.

[23] V.R. Deitz, J.L. Bitner, Interaction of ozone with adsorbent charcoals, Carbon 11 (1973) 339–401.

[24] J. Hoigne, Chemistry of aqueous ozone and transformation of pollutants by ozonation and advanced oxidation processes, in: The Handbook of Environmental Chemistry 5 (Part C), Springer, Berlin, Heidelberg, Germany, 1998.

[25] L. Bernard, P. Bernard, G. Karine, B. Florence, J.P. Croue, Modeling of bromate formation by ozonation of surface waters in drinking water treatment, Water Res. 38 (2004) 2185–2195.

[26] V.K. Pareek, M.P. Brungs, A.A. Adesina, R. Sharma, Artificial neural network modeling of a multiphase photodegradation system, J. Photochem. A 149 (2002) 139–146.

[27] J. Zupan, J. Gasteiger, Neural Networks in Chemistry and Drug Design, Wiley-VCH, Weinheim, 1999.

[28] A. Sozen, E. Arcaklioglu, M. Ozalp, Estimation of solar potential in Turkey by artificial neural networks using meteorological and geographical data, Energy Conver. Manage. 45 (2004) 3033–3052.

[29] M.T. Hagan, H.B. Demuthand, M. Beale, Neural Network Design, PWS Publishing Company, Boston, 1999.

[30] S. Çelik, Ö. Tan, Determination of preconsolidation pressure with artificial neural network, Civil Eng. Environ. Syst. 22 (4) (2005) 217–231.

[31] A. Tortum, The modeling of mode choices of ıntercity freight transportatıon with the artificial neural networks and integrated neuro-fuzzy system, PhD Thesis, Atatürk University, 2003 (in Turkish).